Chemical Physics Letters 595-596 (2014) 230–236

Contents lists available at ScienceDirect

Chemical Physics Letters

journal homepage: www.elsevier.com/locate/cplett

On the formation of ethynylbiphenyl ($C_{14}D_5H_5$; $C_6D_5C_6H_4CCH$) isomers in the reaction of D5-phenyl radicals (C_6D_5; X^2A_1) with phenylacetylene ($C_6H_5C_2H$; X^1A_1) under single collision conditions

Dorian S.N. Parker [a], Tao Yang [a], Ralf I. Kaiser [a,*], Alexander Landera [b], Alexander M. Mebel [b,*]

[a] Department of Chemistry, University of Hawaii at Manoa, Honolulu, HI 96822, United States
[b] Department of Chemistry and Biochemistry, Florida International University, Miami, FL 33199, United States

ARTICLE INFO

Article history:
Received 18 December 2013
In final form 6 February 2014
Available online 14 February 2014

ABSTRACT

Reaction dynamics of the D5-phenyl radical with phenylacetylene were investigated in crossed molecular beams at a collision energy of 120.7 kJ mol^{-1} supported by *ab initio* calculations. The reaction displays indirect, complex forming scattering dynamics, and adduct formation, with D5-phenyl attacking the phenyl ring of phenylacetylene at the ortho, meta and para positions over small entrance barriers. The adduct ($C_6D_5C_8H_6$) undergoes hydrogen emission through tight exit transition states of 34–47 kJ mol^{-1} above the separated products. The phenyl addition–hydrogen elimination mechanism produces various ethynylbiphenyls exoergically by 25–38 kJ mol^{-1}. No phenanthrene was formed under our experimental conditions.

1. Introduction

The investigation of mass growth routes of aliphatic hydrocarbons to (polycyclic) aromatic hydrocarbons (PAHs) from their acyclic precursors in the combustion of fossil fuels is under consistent investigation due to the resultant negative health [1,2] and environmental effects of PAHs [3]. Ideally, a stoichiometric combustion of fossil and bio fuel results in the release of solely water and carbon dioxide, however, the high temperatures and pressures in combustion environments cause fragmentation of the hydrocarbon reactants via carbon–hydrogen and carbon–carbon bond ruptures; these primary radicals subsequently undergo a series of bimolecular reactions [4] mainly with the unsaturated fuel components. These processes are fast and thermodynamically driven towards the formation of polycyclic aromatic hydrocarbons (PAHs) due to their inherent stability, eventually leading to soot particles [4–6]. Some select examples of PAH forming bimolecular reactions are shown in reactions (1)–(5).

The hydrogen abstraction–acetylene addition (HACA) mechanism is one of the earliest, simplest and most well known routes to PAH formation as introduced by Frenklach [7] as well as Bittner and Howard [8]. The high concentrations of phenyl radicals (C_6H_5), benzene (C_6H_6), and acetylene (C_2H_2) [9–13] combined with the high enthalpies of reaction forming PAHs propose the HACA mechanism as a compelling route involved in soot growth in combustion systems [5,14,15]. However, alternative reaction mechanisms have also been proposed. These are, for instance, the ethynyl addition mechanism (EAM) detailed by Kislov et al. [16], which involves mass growth by a series of ethynyl (C_2H) additions and can explain the observation of combustion products with C_2 increment masses. Recently, Parker et al. proposed that PAHs such as indene (C_9H_8), naphthalene ($C_{10}H_8$), and dihydronaphthalene ($C_{10}H_{10}$) can be formed via reactions of phenyl radicals (C_6H_5) with methylacetylene/allene (C_3H_4) [17], vinylacetylene ($HCCC_2H_3$) [18], and 1,3-butadiene ($C_2H_3C_2H_3$) [19], respectively (reactions (1)–(3), with the reactions forming naphthalene ($C_{10}H_8$) and dihydronaphthalene ($C_{10}H_{10}$) being *barrierless*. Lately, focus has been redrawn to the phenyl radical (C_6H_5) and its ability to reach higher-order PAHs through the formation of biphenyl ($C_6H_5C_6H_5$)-type intermediates in what has been coined the phenyl addition–cyclization mechanism (PAC) [20,21]. The concept of PAC, broadly understood as reactive coagulation [22], was prompted by the increased production of complex fused ring structures holding over three benzene rings in benzene flames [12] thought to be formed via incorporation of phenyl radicals and benzene into PAHs [23]. The (self) reaction of phenyl radicals and with benzene has been investigated and proposed to produce PAHs with up to 15 rings as well as large proportions of biphenyl ($C_{12}H_{10}$) [24–26]. Recent crossed beam experiments of the phenyl radical with benzene clearly demonstrated the synthesis of biphenyl ($C_6H_5C_6H_5$) under single collision conditions (reaction (4) [27]. Here, biphenyl present in most combustion flames, has been implicated in PAH formation as an intermediate

* Corresponding authors. Fax: +1 808 956 5908 (R.I. Kaiser).
E-mail address: ralfk@hawaii.edu (R.I. Kaiser).

http://dx.doi.org/10.1016/j.cplett.2014.02.013
0009-2614/

toward acenaphthalene ($C_{12}H_8$) formation involving acetylene and/or ethynyl addition [4,28,29]. The reaction of biphenyl with acetylene (C_2H_2) was theoretically investigated by Mebel et al. to map out the route to phenanthrene formation ($C_{14}H_{10}$) (reaction (5)) [30]. Here, the authors predicted key reaction pathways leading to phenanthrene formation through sequential hydrogen elimination – acetylene addition routes; a second pathway involves molecular hydrogen loss, which is open in high temperature combustion environments. However, with the exception of the formation of the stem compound biphenyl ($C_{12}H_{10}$) [27], elementary reactions of (substituted) biphenyls have not been investigated experimentally to date.

$$C_6H_5 + C_3H_4 \rightarrow C_9H_8 + H \quad (1)$$

$$C_6H_5 + C_4H_4 \rightarrow C_{10}H_8 + H \quad (2)$$

$$C_6H_5 + C_4H_6 \rightarrow C_{10}H_{10} + H \quad (3)$$

$$C_6H_5 + C_6H_6 \rightarrow C_{12}H_{10} + H \quad (4)$$

$$C_{12}H_{10} + C_2H_2 \rightarrow C_{14}H_{10} + 2H \quad (5)$$

In the present study, we access the single collision regime to explore the reaction of phenyl radicals (C_6H_5) with phenylacetylene (C_6H_5CCH). We are combining the phenyl addition approach of the proposed PAC mechanism with the primary product of the HACA mechanism – phenylacetylene (C_6H_5CCH) [31] – a concept previously adopted by Frenklach et al. [4]. Note that this reaction has been investigated previously computationally using density function theory (DFT) at the B3LYP/TZVP and BMK/TZVP levels to map the formation of phenanthrene ($C_{14}H_{10}$), which was found possible over a barrier of 18.8 kJ mol^{-1} utilizing a four-member ring intermediate [32]. However, alternative pathways were not studied; these involve simple phenyl addition–hydrogen atom elimination routes to ethynylbiphenyl isomers. For example, addition of phenyl to the ortho position of phenylacetylene leads to 2-ethynylbiphenyl, which can isomerize thermally to phenanthrene at 900 K [33]. Ethynyl-substituted PAHs, which can be formed through further cyclization of ethynylbiphenyl isomers via the HACA mechanism, might also play host to the thermal formation of cyclopentafused PAHs [34,35], i.e. a class of molecules that is particularly muta- and carcinogenic. Our approach of exploiting crossed molecular beams and combining these studies with high level *ab initio* calculations benefits over existing 'bulk' experimental combustion methods in that we are able to characterize the nascent products and reaction dynamics of a single bimolecular reaction unequivocally. We provide compelling evidence on the synthesis of ethynylbiphenyl isomers – key PAH precursor [30].

2. Methods

2.1. Experimental and data analysis

The reaction of the D5-phenyl radical (C_6D_5; X^2A_1) with phenylacetylene (C_6H_5CCH; X^1A_1) was conducted exploiting a crossed molecular beams machine under single collision conditions [36]. Briefly, a pulsed supersonic beam of D5-phenyl radicals seeded in helium (99.9999 %; Gaspro) at fractions of about 1% was prepared by photodissociation of D5-chlorobenzene (D5-C_6H_5Cl 99.9%; Fluka) in the primary source chamber [17]. This gas mixture was formed by passing 1.5 atm helium gas through D5-chlorobenzene stored in a stainless steel bubbler. The gas mixture was then released by a Proch–Trickl pulsed valve operated at 120 Hz and −400 V and photodissociated by 193 nm light at 10 mJ emitted from a Excimer laser operating at 60 Hz. Note that the laser was fired 40 μs prior to the primary valve. A four-slot chopper wheel located after the skimmer selected a part of the D5-phenyl beam at a peak velocity (v_p) of 1717 ± 20 ms^{-1} with a speed ratio S of S = 12.0 ± 0.2. This section of the radical beam was perpendicularly intersected in the interaction region of the scattering chamber by a pulsed molecular beam of phenylacetylene seeded in a helium carrier gas at 550 torr with fractions of about 1% with peak velocities of 1552 ± 20 ms^{-1} and speed ratio of 8.9 ± 0.2. This gave rise to a collision energy of 120.7 ± 1.6 kJ mol^{-1} and a center-of-mass angle of 49.8 ± 1.0°.

The reactively scattered products were monitored using a triply differentially pumped quadrupole mass spectrometric detector in the time-of-flight (TOF) mode after electron-impact ionization of the neutral species with an electron energy of 80 eV. Time-of-flight spectra were recorded over the full angular range of the reaction in the plane defined by the primary and the secondary reactant beams. The TOF spectra were then integrated and normalized to obtain the product angular distribution in the laboratory frame (LAB). To extract information on the reaction dynamics, the experimental data are transformed into the center-of-mass frame utilizing a forward-convolution routine [37,38]. This method initially assumes an angular flux distribution, $T(\theta)$, and the translational energy flux distribution, $P(E_T)$ in the center-of-mass system (CM). Laboratory TOF spectra and the laboratory angular distributions (LAB) are subsequently calculated from the $T(\theta)$ and $P(E_T)$ functions and compared to the experimental data, the functions are iteratively adjusted until the best fit between the two is achieved.

2.2. Theoretical methods

Geometries of various species involved in the reaction of the phenyl radical with phenylacetylene including intermediates, transition states, and products, were optimized at the hybrid density functional B3LYP level of theory with the 6-311G(d,p) basis set [39]. Vibrational frequencies and zero-point vibrational energy (ZPE) were obtained using the same B3LYP/6-311G(d,p) approach. The optimized geometries of all species were then used in single-point calculations to obtain more accurate energies applying the G3(MP2,CC)//B3LYP modification [40,41] of the original Gaussian 3 (G3) scheme [42]. The final energies at 0 K were obtained using the B3LYP optimized geometries and ZPE corrections according to the following formula:

$$E_0[\mathrm{G3(MP2,CC)}] = E[\mathrm{CCSD}(T)/\mathrm{6\text{-}31G(d,p)}] + \Delta E_{\mathrm{MP2}} + E(\mathrm{ZPE}),$$

where ΔE_{MP2} = E[MP2/G3large] – E[MP2/6-31G(d,p)] is the basis set correction and E(ZPE) is the zero-point energy. ΔE(SO), a spin–orbit correction, and ΔE(HLC), a higher level correction, from the original G3 scheme were not included in our calculations, as they are not expected to make significant contributions into relative energies. The expected accuracy of the G3(MP2,CC)//B3LYP/6-311G(d,p) relative energies is normally within 10 kJ mol^{-1} [41–43]. The Gaussian 09 [43] and Molpro 2006 [44] programs were used for the *ab initio* calculations.

RRKM theory [45] was utilized to compute energy-dependent reaction rate constants of unimolecular reaction steps following the formation of initial adducts under single-collision conditions. Available internal energy for each species, including intermediates and transition states, was taken as the energy of chemical activation plus the collision energy assuming that the latter is dominantly converted into the internal vibrational energy. Harmonic approximation was used for calculations of the density and number of states required to compute the rate constants. Phenomenological first-order rate equations were then solved within the steady-state approximation using the RRKM rate constants to evaluate product branching ratios for decomposition of various initial reaction adducts formed by the addition of phenyl radical to various sites of phenylacetylene.

3. Results

3.1. Laboratory frame

In the bimolecular collision of D5-phenyl radicals (C_6D_5; 82 amu) with phenylacetylene ($C_6H_5C_2H$; 102 amu), signal was collected at three distinct mass-to-charge ratios, m/z, of $m/z = 184$ ($C_6D_5C_8H_6^+/^{13}CC_5D_5C_8H_5^+$), $m/z = 183$ ($C_6D_5C_8H_5^+$), and $m/z = 182$ ($C_6D_4C_8H_6^+/C_6D_5C_8H_4^+$) over the full angular range (Figures 1–4). The signal at $m/z = 184$ corresponds to the formation of an adduct ($C_6D_5C_8H_6$) through recombination of the reactants (Figures 3 and 4). The signal at $m/z = 183$ correlates with the synthesis of a $C_6D_5C_8H_5$ product formed via *atomic hydrogen* emission; since the phenyl radical is fully deuterated, this hydrogen atom must originate from the phenylacetylene molecule (Figures 1 and 2). Signal at $m/z = 182$ was very weak and was found to have superimposable TOF spectra and angular distribution to the signal at $m/z = 183$. We therefore assign signal at $m/z = 182$ to dissociative electron impact ionization of the $C_6D_5C_8H_5$ parent molecule. Note that the laboratory angular distributions shown in Figures 2 and 4 for $m/z = 183$ and 184, respectively, were scaled by the primary beam intensity and averaged over five scans with up to 5120 TOFs each for each angle. Both distributions peak close to the center-of-mass angle of 49.8 ± 0.50° and extend by about 22° ($m/z = 183$) and 18° ($m/z = 184$) in the scattering plane defined by the primary and secondary beams. The peaking of the laboratory angular distribution close to the center-of-mass angle and its symmetric profile in both cases proposes indirect scattering dynamics via the formation of collision complexes with life times longer than their rotational periods [46].

3.2. Center-of-mass frame

Data at $m/z = 183$ ($C_{14}D_5H_5^+$) were fit with a single channel accounting for reactive scattering signal at 183 amu ($C_{14}D_5H_5$) plus 1 amu (H) (Figures 1 and 2). The corresponding center-of-mass translational energy distribution, $P(E_T)$, shown in Figure 5 depicts a maximum translation energy release of 158 ± 16 kJ mol^{-1}. A subtraction of the collision energy of 120.7 ± 1.6 kJ mol^{-1} yields the reaction energy of 38 ± 16 kJ mol^{-1} for those products formed

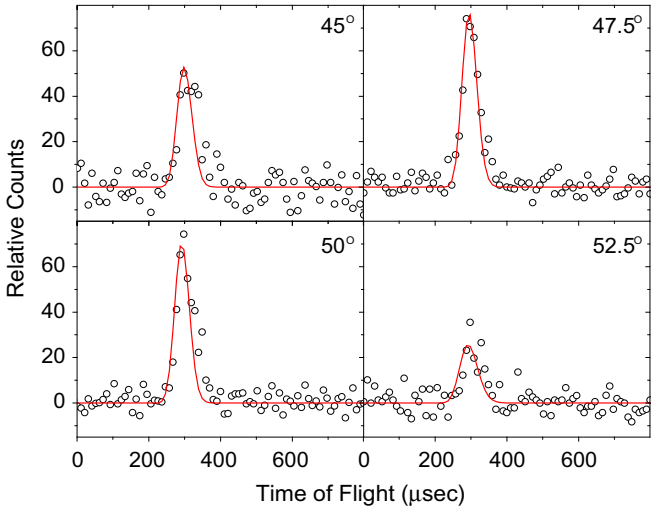

Figure 1. Time-of-flight data at $m/z = 183$ ($C_1D_5H_5^+$) recorded for the reaction of D5-phenyl with phenylacetylene at various laboratory angles at a collision energy of 120.7 kJ mol^{-1}. The circles represent the experimental data, and the solid line represents the fit.

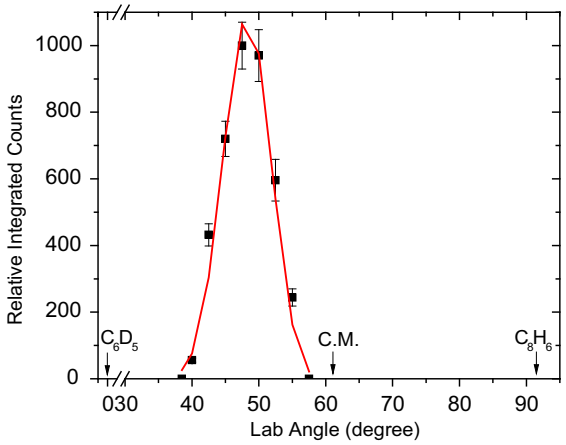

Figure 2. Laboratory angular distribution for the reaction of D5-phenyl plus phenylacetylene recorded at $m/z = 183$ ($C_{14}D_5H_5^+$). Solid squares represent the experimental data together with 1σ error bars.

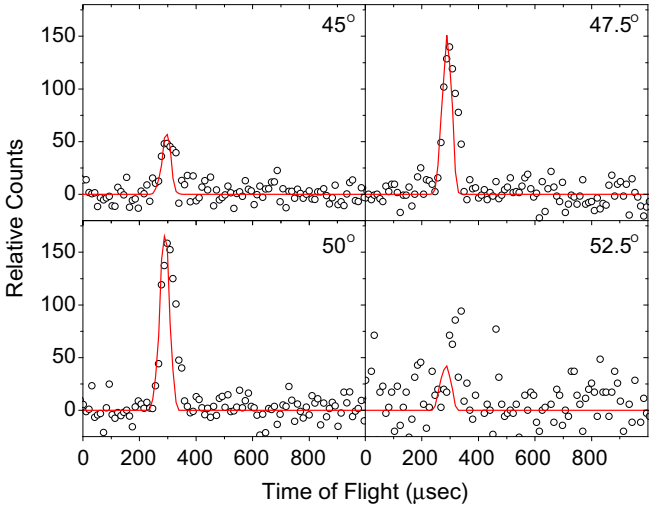

Figure 3. Time-of-flight data at $m/z = 184$ ($C_{14}D_5H_6^+/^{13}CC_{13}D_5H_5^+$) recorded for the reaction D5-phenyl plus phenylacetylene at various laboratory angles at a collision energy of 120.7 kJ mol^{-1}. The circles represent the experimental data, and the solid line represents the fit.

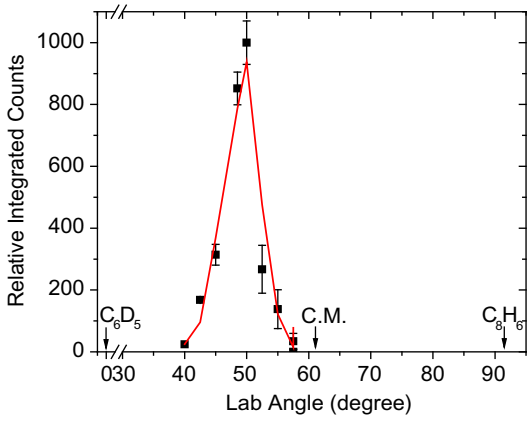

Figure 4. Laboratory angular distribution for the reaction of D5-phenyl with phenylacetylene at $m/z = 184$ ($C_{14}D_5H_6^+/^{13}CC_{13}D_5H_5^+$). The squares represent the experimental data, and the solid line represents the fit.

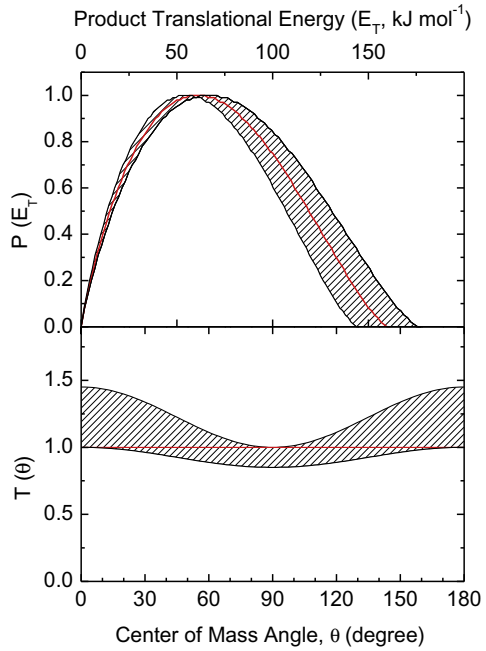

Figure 5. Center-of-mass angular (bottom) and translational energy flux distributions (top) of the reaction of D5-phenyl with phenylacetylene for the atomic hydrogen loss channel at a collision energy of 120.7 kJ mol^{-1}. Hatched areas indicate the acceptable upper and lower error limits of the fits. The red line defines the best fit functions. (For interpretation of the references to colour in this figure legend, the reader is referred to the web version of this article.)

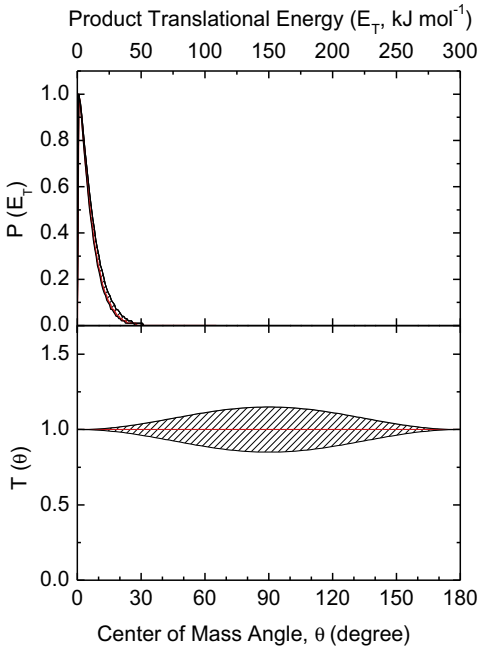

Figure 6. Center-of-mass angular (top) and translational energy flux distributions (bottom) of the reaction of D5-phenyl with phenylacetylene for the adduct at collision energies of 120.7 kJ mol^{-1}. Hatched areas indicate the acceptable upper and lower error limits of the fits. The red line defines the best fit functions. (For interpretation of the references to colour in this figure legend, the reader is referred to the web version of this article.)

without internal excitation. Further, the $P(E_T)$ distribution peaks distinctively away from zero translational energy at about 60 kJ mol^{-1}; this finding suggests the existence of an exit barrier and a tight exit transition state to product formation [46]. Large exit barriers are often associated with repulsive carbon—hydrogen bond ruptures involving a significant electron rearrangement from the decomposing intermediate to the final products. Considering the concept of microscopic reversibility [46], in the reversed reaction of a hydrogen atom addition to a closed shell hydrocarbon, we would expect an entrance energy barrier. Finally, the average fraction of the available energy channeling into the translational degrees of freedom of the products is 70 kJ mol^{-1} which was computed to be 44 ± 6%. Note that the center-of-mass angular distribution, $T(\theta)$, shows intensity over the full angular range indicating an indirect complex forming reaction mechanism forming a $C_6D_5C_8H_6$ intermediate [46]. Best fits are achieved with isotropic (flat), forward–backward distributions indicating that the life time of the decomposing complex is longer than its rotational period [46]. This isotropy is also indicative of a weakly polarized system, in which the initial orbital angular momentum does not couple well with the final orbital angular momentum due to the light mass of the departing hydrogen atom. Considering angular momentum conservation, the initial angular momentum is channeled preferentially into the rotational degrees of freedom of the $C_6D_5C_8H_5$ product(s).

We are turning our attention now to the center-of-mass functions associated with m/z = 184 and shown in Figure 6. Here, a reasonable fit was achieved with one channel and is indicative of adduct formation ($C_6D_5C_8H_6$). Ideally, adduct formation should result only in intensity at the center-of-mass angle with zero translational energy. However, the angular and velocity spreads of both beams result in a broader range of scattering angles. Previously, adducts have been observed in the crossed beam reactions of boron [47], carbon [48], and oxygen atoms [49] with benzene. The detection of the adduct ($C_6D_5C_8H_6$) indicates that the reaction of the D5-phenyl radical with phenylacetylene proceeds via an indirect reaction mechanism under these collision conditions.

3.3. Theoretical results

The $C_6D_5C_8H_6$ potential energy surface (PES) is compiled in Figure 7. Our calculations show that the D5-phenyl radical adds to either the terminal carbon atom of the ethynyl unit (Figure 7A) or to the o, m, or p-position(s) of the benzene ring (Figure 7B and C) leading to intermediates [i1], [i6], [i10], and [i11], respectively. Let us focus on the addition to the ethynyl unit first. This pathway is associated with a significant entrance barrier of 14 kJ mol^{-1}, which can be overcome at our collision energy of 121 ± 2 kJ mol^{-1}. Intermediate [i1] is stabilized by 188 kJ mol^{-1} with respect to the reactants and can lose a hydrogen atom forming D5-diphenylacetylene ($C_6D_5CCC_6H_5$) [p2] in an overall exoergic reaction (−51 kJ mol^{-1}) through a tight exit transition state located 31 kJ mol^{-1} above the energy of the separated reactants. The initial collision complex [i1] can alternatively undergo a hydrogen migration from the phenyl ring to the acetyl group to form [i2], a trans-diphenylethene type structure; the latter is able to isomerize to its cis conformer [i4] through a two-step mechanism involving a closure and opening of a four-member ring via the intermediate [i3], with highest in energy transition state positioned 157 kJ mol^{-1} above [i2]. Alternatively, [i4] can be formed directly from [i2] by rotation around the double C═C bond, but the barrier for this process is even higher between at 208 kJ mol^{-1}. Once intermediate [i4] is reached, a relatively small barrier of 17 kJ mol^{-1} to cyclization is overcome to reach intermediate [i5]. This isomer represents the lowest in energy minimum of the investigated potential energy surface and can undergo atomic hydrogen emission from the sp^3 hybridized carbon to reach the phenanthrene molecule [p1] with an overall reaction exoergicity of 247 kJ mol^{-1}.

Figure 7B shows the potential energy surface accessed through the addition of the phenyl radical to the ortho position

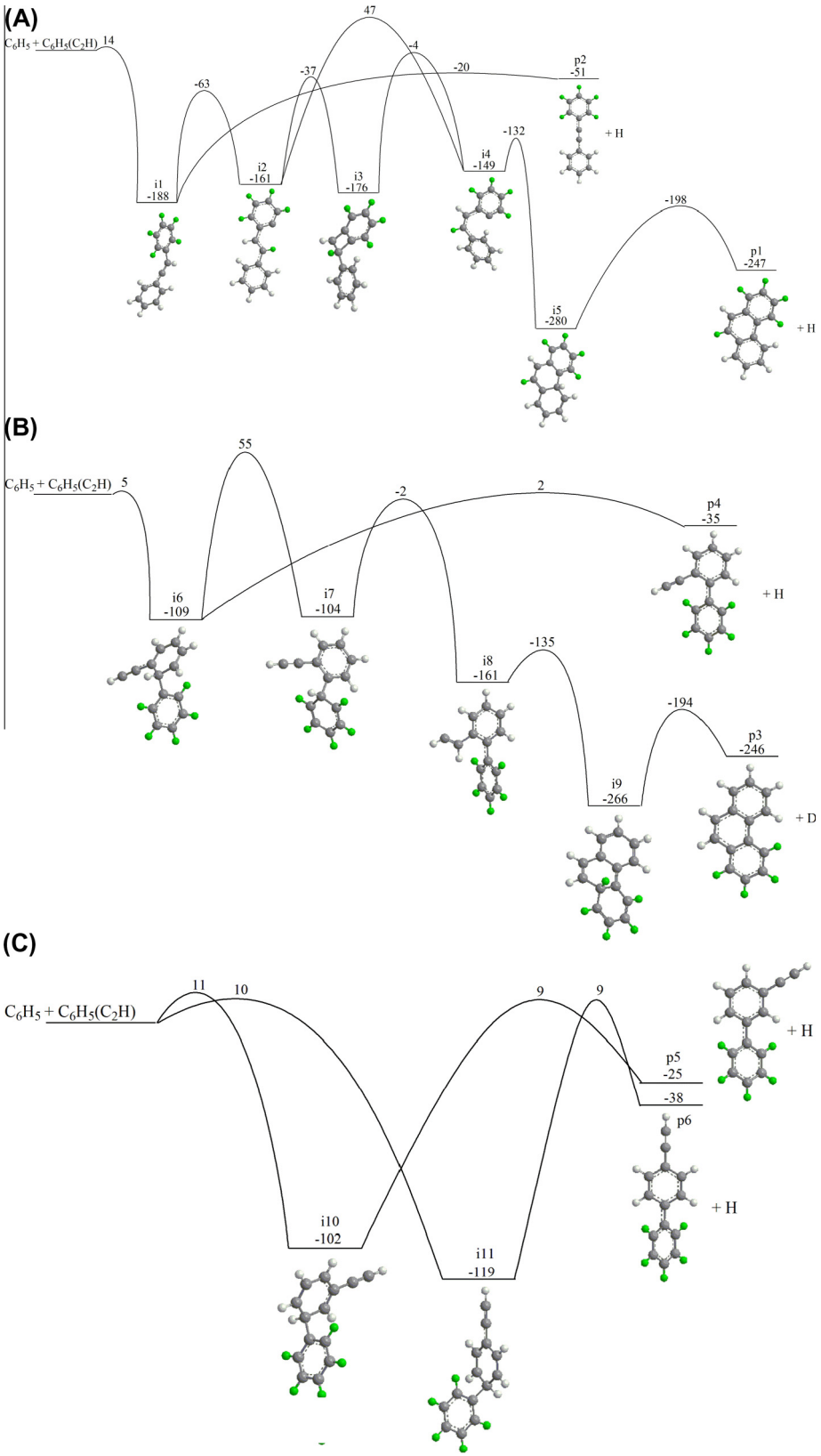

Figure 7. Schematic representation of the $C_6D_5C_8H_6$ potential energy surface (PES) accessed via the reaction of D5-phenyl (X^2A_1) with phenylacetylene (X^1A_1). (A) Phenyl addition to the acetylic group of phenylacetylene, (B) phenyl addition to the ortho carbon of phenylacetylene molecule, (C) phenyl addition to the meta and para carbons of phenylacetylene. Atom designations: carbon – gray, hydrogen – white, deuterium – green. Relative energies are in kJ mol^{-1} and calculated at the G3(MP2,CC)//B3LYP/6–311G(d,p) level.

of phenylacetylene. This addition has a low entrance barrier of 5 kJ mol^{-1} and reaches the intermediate [i6], which resides in a potential energy well of 109 kJ mol^{-1} relative to the separated reactants. From intermediate [i6], hydrogen emission from the ortho carbon of phenylacetylene reaches 2-ethynylbiphenyl [p4] with an overall reaction exoergicity of 35 kJ mol^{-1}. Hydrogen migration in intermediate [i6] has a large energy barrier of 164 kJ mol^{-1} and leads to intermediate [i7]. Further hydrogen migration from the phenyl ring to the acetyl group over a barrier of 106 kJ mol^{-1} leads to intermediate [i8]. Cyclization provides a tricyclic intermediate [i9]. Emission of the out-of-plane hydrogen atom from intermediate [i9] over a barrier of 72 kJ mol^{-1} accesses the phenanthrene product [p3] in an overall exoergic reaction (−246 kJ mol^{-1}).

Figure 7C compiles the addition routes by phenyl to the meta and para positions of phenylacetylene yielding intermediates [i10] and [i11] via moderately low entrance barriers of 11 and 10 kJ mol^{-1}, respectively. These collision complexes cannot be connected to phenanthrene. Instead, intermediates [i10] and [i11] undergo hydrogen emission from the meta and para carbon of the phenylacetylene unit 3-ethynylbiphenyl [p5] and 4-ethynylbiphenyl [p6], respectively. These products are formed through tight exit transition states located 34 and 47 kJ mol^{-1} above the energies of the separated products in overall exoergic reactions of 25 and 38 kJ mol^{-1}, respectively.

4. Discussion

We will now combine our experimental findings with the potential energy surfaces to elucidate the reaction dynamics in the reaction of D5-phenyl radicals with phenylacetylene conducted at a collision energy of about 121 kJ mol^{-1}. The experimental data showed explicitly that two channels exist: firstly adduct formation [$C_6D_5C_8H_6$; m/z = 184] and secondly, and most significantly, a reaction channel forming a product with the molecular formula $C_6D_5C_8H_5$ (m/z = 183) through a phenyl radical–hydrogen atom exchange mechanism; no deuterium atom emission has been observed experimentally. First, the detection of the adduct provides explicit evidence that the $C_6D_5C_8H_6$ molecule has a life time longer than its flight time of 26 μs from the collision center in the scattering machine to the ionizer of the detector. Further, indirect scattering dynamics of the reactive scattering channel is evident. Second, with respect to the phenyl radical–hydrogen exchange pathway and inherent formation of the $C_6D_5C_8H_5$ product(s), the exoergicity of 38 ± 16 kJ mol^{-1} matches well the calculated energies to form the 2-, 3- and 4-ethynylbiphenyl isomers (p4, p5, and p6) predicted to be formed with reaction exoergicities of 35, 25, and 38 kJ mol^{-1}. There is no evidence of phenanthrene formation under our experimental conditions; the reaction energy of 246 kJ mol^{-1} is a factor of 5 times greater than the experimentally derived reaction energy. It should be noted that phenanthrene formation competes with a phenyl addition – atomic hydrogen elimination channel leading to 2-ethynylbiphenyl [p4] (Figure 7). The energy barriers to isomerization of [i6] between the two channels range from 55 to 2 kJ mol^{-1} above the energy of the separated reactants; therefore, [i6] prefers decomposition to 2-ethynylbiphenyl [p4] rather than isomerizing to [i7]. Note that the formation of biphenylacetylene is also possible under our experimental conditions considering the reaction exoergicity of 51 kJ mol^{-1} being on the error boundaries of our experimental data that reach to 54 kJ mol^{-1}. We conclude that biphenylacetylene [p2] could be formed, but to a minor extent and not as the predominant reaction pathway, which favors a reaction energy close to 38 kJ mol^{-1}. Recall that no atomic deuterium loss was observed. Figure 7B depicts a feasible deuterium loss pathway to form phenanthrene (p3). However, the reaction energy cannot be matched by our experimental data. Therefore, the lack of any deuterium atom emission also verified that phenanthrene is not formed in our experiment under single collision conditions. It should also be noted that reference mass spectra of phenanthrene under hard electron ionization conditions show that the phenanthrene ion would stay intact with it being the dominant mass peak by 80% [50]. The lack of formation of phenanthrene is also supported by RRKM theory, which finds that only the non-PAH products ethynylbiphenyl and biphenylacetylene are formed. The results show that the unimolecular decomposition of the energized [i1] adduct should produce only biphenylacetylene [p2], whereas the dissociation of [i6], [i10], and [i11] leads to the exclusive formation of 2-, 3-, and 4-ethynylbiphenyls, [p4], [p5], and [p6], respectively. Hence, the branching ratios of the ethynylbiphenyl and biphenylacetylene products would be mostly controlled by branching of the reaction flow in the entrance channel, i.e., by the site of phenyl addition to phenylacetylene. Under single-collision conditions the entrance channel branching is determined by reaction cross sections at a particular collision energy. However, a crude evaluation of relative importance of the different addition channels can be made by calculating their bimolecular rate constants at a temperature at which the average kinetic energy is equal to the collision energy, here at 9678 K. Such calculations show that 83% of the reaction flux goes through ortho addition, 11% goes through para addition, 5% goes through meta addition, and the remaining 1% goes through side chain addition, which correlates well with the barrier heights for the respective entrance channels. Based on this, 2-ethynylbiphenyl should be expected as the dominant reaction product, with minor contributions from 4- and 3-ethynylbiphenyl and only a trace yield of biphenylacetylene. It should be also noted that the theoretical branching ratios exhibit very weak dependence on the collision energy up to 120.7 kJ mol^{-1}.

Having proposed the products to be 2-ethynylbiphenyl, 3-ethynylbiphenyl, and/or 4-ethynylbiphenyl ($C_6D_5C_8H_5$) plus atomic hydrogen, we imply the following reaction dynamics. The reaction of the phenyl radical with phenylacetylene is dictated by indirect scattering dynamics and initiated by the addition of the phenyl radical with its radical center to the o-, m-, and/or p-positions of the phenylacetylene molecule via small barriers of about 5–11 kJ mol^{-1} leading to the formation of [i6], [i10], and/or [i11]. A fraction of these collision complexes have a life time long enough to fly to the detector of the crossed beams machine (>26 μs) to be ionized in the electron impact ionizer. These intermediates also decompose via atomic hydrogen elimination forming 2-ethynylbiphenyl, 3-ethynylbiphenyl, and/or 4-ethynylbiphenyl ($C_6D_5C_8H_5$) via tight exit transition states located 34–47 kJ mol^{-1} above the separated products. No atomic deuterium loss was observed verifying that the formation of phenanthrene (p1) is prohibited through phenyl addition at the ortho position.

5. Summary

The reaction of the D5-phenyl radical (C_6D_5; X^2A_1) with phenylacetylene ($C_6H_5C_2H$; X^1A_1) was investigated at a collision energy of about 121 kJ mol^{-1} exploiting the cross molecular beam technique and supported by *ab initio* calculations. The reaction proceeds indirectly via the formation of $C_6D_5C_8H_6$ collision complexes through addition of the phenyl radical to the o-, m-, and/or p-positions of the phenylacetylene molecule via small barriers of about 5–11 kJ mol^{-1}. A part of these collision complexes hold life times long enough to fly to the detector of the crossed beams machine. The collision complexes also undergo unimolecular decomposition via atomic hydrogen elimination leading to 2-ethynylbiphenyl, 3-ethynylbiphenyl, and/or 4-ethynylbiphenyl ($C_6D_5C_8H_5$) via tight exit transition states in overall slightly exoergic reactions of typically

34–47 kJ mol^{-1}. No atomic deuterium loss was observed proposing that phenanthrene was not formed. Recall that the reaction of the phenyl radical with phenylacetylene has previously been investigated by electronic structure calculations and suggested to reach phenanthrene – a prototypical tricyclic PAH [32]. This is contrary to our findings in which we see no phenanthrene formation in any appreciable quantities under single collision conditions. However, it should be noted that 2-ethynylbiphenyls have been shown to easily form phenanthrene through thermalization at 900 K [33]. Furthermore, substituted biphenyls have been implicated as intermediates in rapid mass growth routes through the PAC mechanism forming high order PAHs.

Acknowledgments

This work was supported by the US Department of Energy, Basic Energy Sciences (Grants No. DE-FG02-03ER15411 to R.I.K. and the University of Hawaii and DE-FG02-04ER15570 to A.M.M. at FIU).

References

[1] M.F. Denissenko, A. Pao, M.-S. Tang, G.P. Pfeifer, Science (Washington, DC) 274 (1996) 430.
[2] W.M. Baird, L.A. Hooven, B. Mahadevan, Environ. Mol. Mut. 45 (2005) 106.
[3] B.J. Finlayson-Pitts, J.N. Pitts Jr., Science (New York, NY) 276 (1997) 1045.
[4] M. Frenklach, Phys. Chem. Chem. Phys. 4 (2002) 2028.
[5] V.V. Kislov, A.I. Sadovnikov, A.M. Mebel, J. Phys. Chem. A 117 (2013) 4794.
[6] H. Richter, J.B. Howard, Prog. Energy Combust. Sci. 26 (2000) 565.
[7] M. Frenklach, D.W. Clary, W.C. Gardiner, S.E. Stein, Proc. Int. Symp. Combust. 20 (1985) 887.
[8] J.D. Bittner, J.B. Howard, Proc. Int. Symp. Combust. 18 (1981) 1105.
[9] Y. Li, L. Zhang, Z. Tian, T. Yuan, J. Wang, B. Yang, F. Qi, Energy Fuels 23 (2009) 1473.
[10] T.R. Melton, F. Inal, S.M. Senkan, Combust. Flame 121 (2000) 671.
[11] T.R. Melton, A.M. Vincitore, S.M. Senkan, Symp. (Int.) Combust. [Proc.] 27 (1998) 1631.
[12] H. Richter, T.G. Benish, O.A. Mazyar, W.H. Green, J.B. Howard, Proc. Combust. Inst. 28 (2000) 2609.
[13] B. Yang, Y. Li, L. Wei, C. Huang, J. Wang, Z. Tian, R. Yang, L. Sheng, Y. Zhang, F. Qi, Proc. Combust. Inst. 31 (2007) 555.
[14] C.W. Bauschlicher Jr., A. Ricca, Chem. Phys. Lett. 326 (2000) 283.
[15] V.V. Kislov, N.I. Islamova, A.M. Kolker, S.H. Lin, A.M. Mebel, J. Chem. Theory Comput. 1 (2005) 908.
[16] A.M. Mebel, V.V. Kislov, R.I. Kaiser, J. Am. Chem. Soc. 130 (2008) 13618.
[17] D.S.N. Parker, F. Zhang, R.I. Kaiser, V.V. Kislov, A.M. Mebel, Chem. Asian J. 6 (2011) 3035.
[18] D.S.N. Parker, F. Zhang, Y.S. Kim, R.I. Kaiser, A. Landera, V.V. Kislov, A.M. Mebel, A.G.G.M. Tielens, Proc. Natl. Acad. Sci. 109 (2012) 53.
[19] R.I. Kaiser, D.S.N. Parker, F. Zhang, A. Landera, V.V. Kislov, A.M. Mebel, J. Phys. Chem. A 116 (2012) 4248.
[20] B. Shukla, M. Koshi, Combust. Flame 158 (2011) 369.
[21] B. Shukla, K. Tsuchiya, M. Koshi, J. Phys. Chem. A 115 (2011) 5284.
[22] N.M. Marinov, W.J. Pitz, C.K. Westbrook, M.J. Castaldi, S.M. Senkan, Combust. Sci. Tech. 116–117 (1996) 211.
[23] H. Richter, W.J. Grieco, J.B. Howard, Combust. Flame 119 (1999) 1.
[24] E. Heckmann, H. Hippler, J. Troe, Symp. (Int.) Combust. [Proc.] 26 (1996) 543.
[25] R.S. Tranter, S.J. Klippenstein, L.B. Harding, B.R. Giri, X. Yang, J.H. Kiefer, J. Phys. Chem. A 114 (2010) 8240.
[26] A. Comandini, T. Malewicki, K. Brezinsky, J. Phys. Chem. A 116 (2012) 2409.
[27] F. Zhang, X. Gu, R.I. Kaiser, J. Chem. Phys. 128 (2008) 084315/1.
[28] M. Frenklach, D.W. Clary, W.C. Gardiner, S.E. Stein, Proc. Combust. Inst. 21 (1986) 1067.
[29] M. Frenklach, T. Yuan, M.K. Ramachandra, Energy Fuels 2 (1988) 462.
[30] V.V. Kislov, A.M. Mebel, S.H. Lin, J. Phys. Chem. A 106 (2002) 6171.
[31] X. Gu, F. Zhang, Y. Guo, R.I. Kaiser, Angew. Chem. Int. Ed. 46 (2007) 6866.
[32] J. Aguilera-Iparraguirre, W. Klopper, J. Chem. Theory Comput. 3 (2007) 139.
[33] I.D. Mackie, R.P. Johnson, J. Org. Chem. 74 (2009) 499.
[34] J. Cioslowski, M. Schimeczek, P. Piskorz, D. Moncrieff, J. Am. Chem. Soc. 121 (1999) 3773.
[35] J. Hofmann, G. Zimmermann, K. Guthier, P. Hebgen, K.-H. Homann, Liebigs Annalen (1995) 631.
[36] R.I. Kaiser, P. Maksyutenko, C. Ennis, F. Zhang, X. Gu, S.P. Krishtal, A.M. Mebel, O. Kostko, M. Ahmed, Faraday Discuss. 147 (2010) 429.
[37] M. Vernon, PhD Thesis, University of California, Berkeley, CA, 1981.
[38] M.S. Weiss, PhD Thesis, University Of California, Berkeley, CA, 1986.
[39] P.J. Stephens, F.J. Devlin, M.J. Frisch, C.F. Chabalowski, J. Phys. Chem. 98 (1994) 11623.
[40] A.G. Baboul, L.A. Curtiss, P.C. Redfern, K. Raghavachari, J. Chem. Phys. 110 (1999) 7650.
[41] L.A. Curtiss, K. Raghavachari, P.C. Redfern, A.G. Baboul, J.A. Pople, Chem. Phys. Lett. 314 (1999) 101.
[42] L.A. Curtiss, K. Raghavachari, P.C. Redfern, V. Rassolov, J.A. Pople, J. Chem. Phys. 109 (1998) 7764.
[43] Frisch, M.J. et al., Gaussian 98, Revision A.11, Gaussian Inc. Wallingford, CT (2004).
[44] Werner, H.-J. et al., Molpro, Version 2006.1, MOLPRO, 2006.
[45] J. Steinfield, J. Francisco, W. Hase, Chemical Kinetics and Dynamics, Prentice Hall, Englewood Cliffs, NJ, 1989.
[46] R.D. Levine, Molecular Reaction Dynamics, Cambridge University Press, Cambridge, 2005.
[47] H.F. Bettinger, R.I. Kaiser, J. Phys. Chem. A 108 (2004) 4576.
[48] I. Hahndorf, Y.T. Lee, R.I. Kaiser, L. Vereecken, J. Peeters, H.F. Bettinger, P.R. Schreiner, P.v.R Schleyer, W.D. Allen, H.F. Schaefer III, J. Chem. Phys. 116 (2002) 3248.
[49] D.S.N. Parker, F. Zhang, R.I. Kaiser, J. Phys. Chem. A 115 (2011) 11515.
[50] P.J. Linstrom, W.G. Mallard, NIST Chemistry WebBook, NIST Chemistry WebBook. NIST Standard Reference, Database Number 69.